J. Fluid Mech. (1965), *vol.* 23, *part* 2, *pp.* 305–314
Printed in Great Britain

The three-dimensional laminar boundary layer on a rotating helical blade

By J. H. HORLOCK AND J. WORDSWORTH
Mechanical Engineering Department, University of Liverpool

(Received 11 December 1963 and in revised form 31 December 1964)

The equations of motion of an incompressible viscous fluid are given in a rotating helical co-ordinate system, which is non-orthogonal. Partial differential equations are derived for the boundary-layer flow on a rotating helical blade. Numerical solutions of these equations show that the radial flow in the boundary layer is strongly dependent upon the stagger and speed of rotation of the blade.

1. Introduction

The boundary-layer flow over the blades of an axial-flow turbomachine is not two-dimensional. On the stationary blades the boundary layer is usually subject to a radial pressure gradient (pressure increasing with radius) which arises because of the circumferential component of velocity in the mainstream flow. Because of viscous effects, the velocity near the blades is less than that in the mainstream and an inward radial movement of fluid results. On the rotating blades the fluid near the surface of the blade may move faster than that in the mainstream and, if so, it may move radially outward, even if the pressure increases with radius in the mainstream. If the blade is inclined at an angle $\psi(\neq 0)$ to the axis of rotation, Coriolis forces may also be important.

Two special cases studied previously may be mentioned here:

(i) A blade rotating in a fluid at rest. Fogarty (1951) has studied the laminar boundary-layer flow on a semi-infinite flat plate rotating about an axis perpendicular to its plane and passing through its edge. Mainstream pressure gradients are absent, but Coriolis effects are important, for the angle ψ approaches 90°. The fluid is centrifuged outwards. From the Navier–Stokes equations, referred to a set of rotating axes, Fogarty derived the Blasius equation for flow along the chord, and a second equation for flow along the span. Numerical solutions were obtained.

(ii) A stationary blade of high stagger ($\psi = 90°$). Mager & Hansen (1952) have derived equations for the inward radial flow of the boundary layer on a semi-infinite flat plate when the streamlines outside the boundary layer are of circular shape. Numerical solutions were obtained for the radial velocity.

For the study of the boundary layers on turbine and compressor blades, a co-ordinate system more general than those used by Fogarty and Mager & Hansen is required, because the mainstream flow follows a path which is approximately helical. Figure 1 shows the helical co-ordinate system chosen for the present investigation. The helical blade has its leading edge along the radial

line marked ξ in figure 1. The helix x is a typical generator of the blade; its radius and angle are z and ψ respectively, and, when its initial point is moved along the radial line ξ, the helix itself traverses the surface of the blade. A general point P_b on the blade has co-ordinates (x, z), where x represents the distance of P_b from the leading edge measured along the helix, and z represents the distance from the axis of rotation. A general point P_f in the flow has co-ordinates (x, y, z), where y denotes the distance between P_b and P_f measured along the helix orthogonal to the blade. The co-ordinates (x, y, z) form a non-orthogonal system, the curves along which x, y and z separately increase being respectively a helix of angle ψ drawn on a cylinder of radius z, the helix of angle $(270° + \psi)$ on the same cylinder, and the straight line normal to the cylinder. The corresponding velocity components relative to the co-ordinate system are denoted by (u, v, w). Use of such a co-ordinate system, rotating with angular velocity Ω about the ζ axis, enables a general analysis for the laminar boundary layers on helical blades to be developed. The cases studied by Fogarty and Mager & Hansen are then particular examples of the use of this general analysis.

The momentum equation in a system rotating with angular velocity Ω has been given, for example, by Mager (1954); it is

$$\nabla(\tfrac{1}{2}q^2) - \mathbf{q} \times (\nabla \times \mathbf{q}) + 2(\boldsymbol{\Omega} \times \mathbf{q}) + (\boldsymbol{\Omega} \times (\boldsymbol{\Omega} \times \mathbf{r})) = -(1/\rho)\nabla p - \nu(\nabla \times (\nabla \times \mathbf{q})). \quad (1)$$

The continuity equation for incompressible flow is

$$\nabla . \mathbf{q} = 0, \quad (2)$$

where $\mathbf{q}$ is the velocity relative to the rotating system, p the pressure, ρ the density and $\mathbf{r}$ the position vector relative to the origin O (see figure 1). The momentum equations in the x-, y- and z-directions of the rotating helical co-ordinate system are given in the appendix, together with the continuity equation.

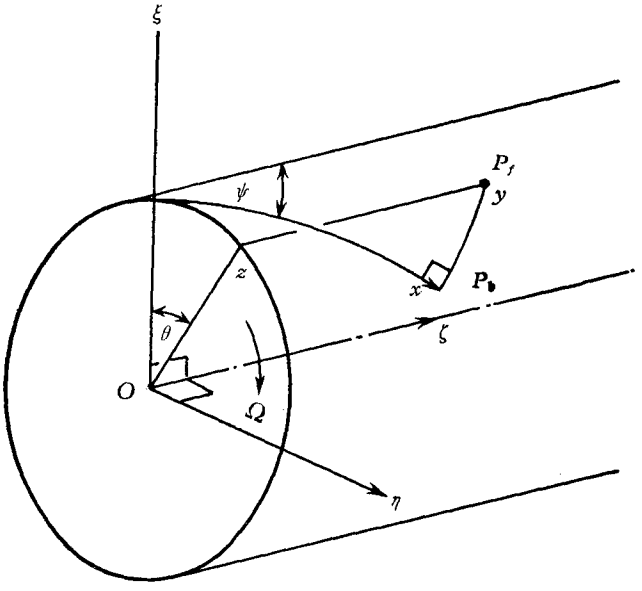

FIGURE 1. The helical co-ordinate system.

2. The boundary-layer equations

The equations of motion given in the appendix are used as the starting-point of a study of the boundary-layer flow on a helical blade lying in the surface $y = 0$ (see figure 2). Here, as in an axial turbomachine, the fluid flows in an annular region between an inner cylinder C_1, rotating about the ζ-axis, and an outer fixed cylinder C_2; the helical blade projects from the surface of C_1. The annular wall boundary layers on C_1 and C_2 are not considered in this problem, it being supposed that they do not interfere with the boundary layer developed on the rotating blade.

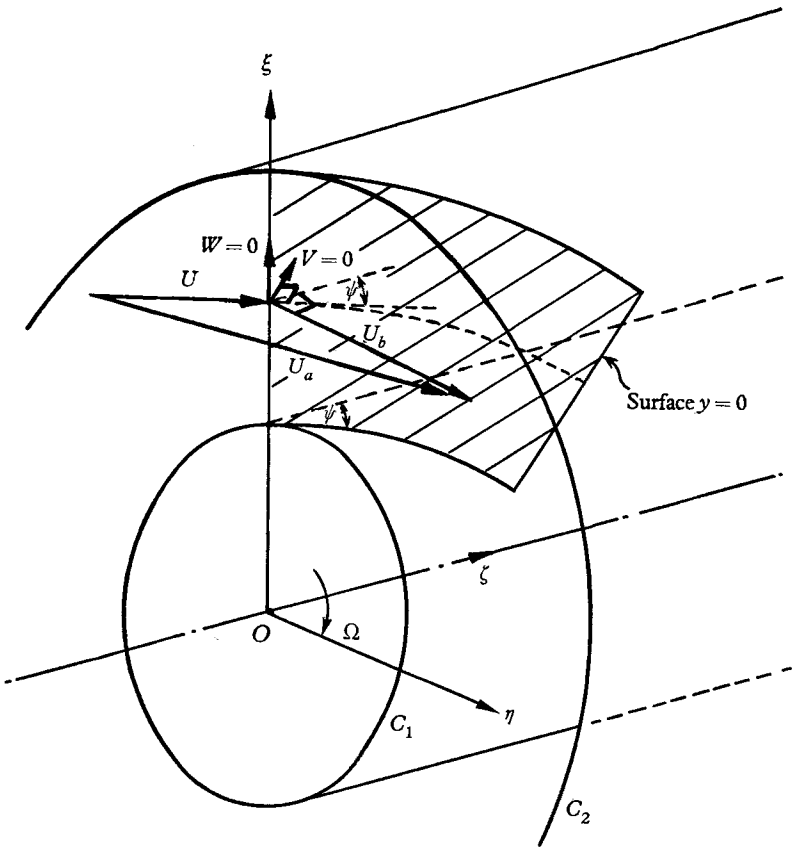

FIGURE 2. The helical blade. $\mathbf{U}$ = relative velocity at entry; $\mathbf{U}_b$ = blade speed; $\mathbf{U}_a = (\mathbf{U}+\mathbf{U}_b)$; $\mathbf{V} = \mathbf{W} = 0$.

The mainstream flow in the annular region has axial and circumferential components of velocity. When the blade speed $\mathbf{U}_b = (\boldsymbol{\Omega} \times \mathbf{z})$ is subtracted from the absolute velocity $\mathbf{U}_a = (\mathbf{U}_b + \mathbf{U})$, the resultant relative velocity $\mathbf{U}(z)$ is parallel to the blade. This condition of zero incidence approximates to the design condition in most turbomachines.

The axial component of absolute velocity is thus $U\cos\psi$, and the circumferential component is $(U_b + U\sin\psi)$. It is assumed that this mainstream flow is in radial equilibrium, i.e. that the radial velocity is zero. Outside the boundary layer the components of velocity relative to the rotating system (x, y, z) are then

$$U = U(z), \quad V = 0, \quad W = 0, \tag{3}$$

since the flow is at zero incidence, and has no radial component.

Equations (31), (32), (33) and (34) of the appendix, which will be solved for constant z, may be made non-dimensional by dividing all lengths by the maximum length of the blade in the x-direction (c), velocities by the mainstream velocity U, angular velocity by (U/c), pressure by ρU^2, and kinematic viscosity by Uc. Dimensional symbols already defined are retained for the non-dimensional analysis that follows below.

The velocity distribution of equation (3) implies that the pressure in the mainstream depends only on z, and is given by

$$\frac{dp}{dz} = \frac{(U\sin\psi + \Omega z)^2}{z}, \tag{4}$$

as can be established from the equations of motion, or otherwise.

Some assumptions are now made which simplify the equations of motion within the boundary layer:

(i) The boundary-layer thickness is small with the chord; thus in the boundary layer $y = O(\delta)$, where $\delta \ll 1$.

(ii) The ratio of the length of the blade to the radius is small, or $z = O(1/\epsilon)$, where $\epsilon \ll 1$.

(iii) The blade speed and mainstream velocity are of like order, as in conventional turbomachines, i.e.

$$\Omega z/U = O(1) \quad \text{or} \quad \Omega = O(\epsilon).$$

It follows from (i) and (ii) that

$$\theta = (x\sin\psi - y\cos\psi)/z$$

is small, $\theta = O(\delta)$ or $\theta = O(\epsilon)$, whichever is the greater, and from (ii) and (iii) that the mainstream radial pressure gradient is small, i.e. $dp/dz = O(\epsilon)$. The curvature of the blade ($k = (\sin\psi)^2/z$) is also $O(\epsilon)$.

At the leading edge of the blade the radial velocity w is zero. The development of radial flow within the boundary layer will be controlled by the angular velocity, the mainstream pressure gradient, and the curvature of the blade, and these have been assumed to be small, so that $w = O(\epsilon)$. Terms in a small quantity of relative order higher than the first are now neglected in the equations of motion (see appendix). The continuity equation (34) becomes

$$\frac{\partial u}{\partial x} + \frac{\partial v}{\partial y} = 0, \tag{5}$$

and, since u and $\partial u/\partial x$ are $O(1)$, $\partial v/\partial y$ is $O(1)$, v is $O(\delta)$.

It can be seen from the momentum equation in the y-direction (equation (32)) that the pressure is sensibly constant across the boundary layer, so that the

mainstream pressure distribution is imposed on the boundary layer. The momentum equation in the x-direction (equation (31)) is therefore

$$u\frac{\partial u}{\partial x}+v\frac{\partial u}{\partial y}-\nu\frac{\partial^2 u}{\partial y^2}=0, \tag{6}$$

and the momentum equation in the z-direction (equation (33)) is

$$u\frac{\partial w}{\partial x}+v\frac{\partial w}{\partial y}+\frac{(U^2-u^2)\sin^2\psi}{z}+2(U-u)\,\Omega\sin\psi-\nu\frac{\partial^2 w}{\partial y^2}=0. \tag{7}$$

The Reynolds number based on the blade length is

$$R_e=(1/\nu)=O(\delta^{-2}). \tag{8}$$

3. Solutions of the differential equations

The differential equations (5), (6) and (7) describe, to a first order, the boundary-layer flow on a rotating helical blade. The equations cannot be solved analytically and methods suggested by Blasius (1908) and Fogarty (1951) are used to obtain numerical solutions.

Following Blasius, a stream function ϕ is introduced which satisfies the continuity equation (5):

$$u=\frac{\partial\phi}{\partial y},\quad v=-\frac{\partial\phi}{\partial x}. \tag{9}$$

By defining
$$\phi=(\nu Ux)^{\frac{1}{2}}f(\eta), \tag{10}$$

and
$$\eta=y(U/\nu x)^{\frac{1}{2}}, \tag{11}$$

it follows that
$$u=Uf', \tag{12}$$

$$v=\tfrac{1}{2}(\nu U/x)^{\frac{1}{2}}(\eta f'-f). \tag{13}$$

Equation (6) then becomes the Blasius equation

$$2f'''+ff''=0, \tag{14}$$

with boundary conditions

$$\left.\begin{matrix}f=0\\f'=0\end{matrix}\right\}\quad\text{at}\quad\eta=0,\quad f'=1\quad\text{at}\quad\eta=\infty. \tag{15}$$

A numerical solution of the Blasius equation has been given by Howarth (1938); he found that

$$f''(0)=0{\cdot}33206. \tag{16}$$

The equation of motion in the radial direction is reduced by making a substitution similar to that suggested by Fogarty,

$$w=xU\lambda/z. \tag{17}$$

Equation (7) then becomes

$$2\lambda''+\lambda' f-2\lambda f'-2P^2(1-f'^2)-4PQ(1-f')=0, \tag{18}$$

in which
$$P=\sin\psi,\quad Q=z\Omega/U. \tag{19}$$

Equation (18) may be solved by setting

$$\lambda = P\{Pg(\eta) + Qh(\eta)\}, \tag{20}$$

where

$$2g'' + g'f - 2gf' - 2(1 - f'^2) = 0, \tag{21}$$

$$2h'' + h'f - 2hf' - 4(1 - f') = 0. \tag{22}$$

The boundary or conditions on (21) and (22) are

$$\left.\begin{aligned} f &= 0, \\ f' &= 0, \\ f'' &= 0{\cdot}33206, \\ g &= 0, \\ h &= 0, \end{aligned}\right\} \quad \text{at} \quad \eta = 0, \quad \left.\begin{aligned} g &= 0, \\ h &= 0, \end{aligned}\right\} \quad \text{at} \quad \eta = \infty. \tag{23}$$

Numerical solutions of equations (21) and (22) were obtained using a digital computer. The initial slope of the curve $g = g(\eta)$ (or $h = h(\eta)$) at the origin was guessed and g (or h) obtained at equal intervals of η, using the Runge-Kutta method with interval $\Delta\eta = 0{\cdot}2$ for $0 \leqslant \eta < 8$. The correct initial slope $g'(0)$ (or $h'(0)$) to give $g \to 0$ (or $h \to 0$) as $\eta \to \infty$ was found by trial and error. Solutions of equations (21) and (22) are given in figure 3.

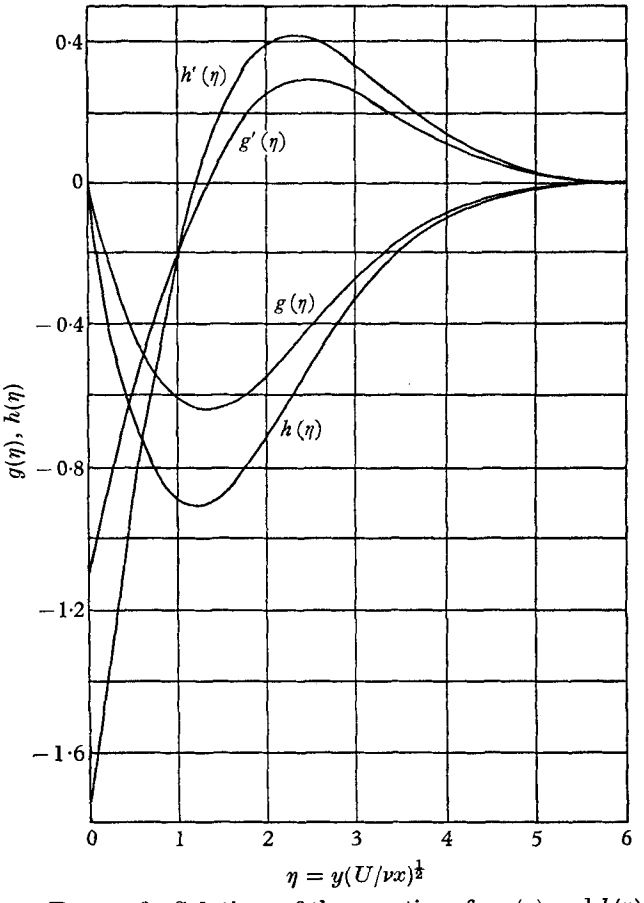

FIGURE 3. Solutions of the equations for $g(\eta)$ and $h(\eta)$.

It is of interest to determine the angular displacement of the boundary-layer flow from the x-direction. This angle is defined as

$$\gamma = \tan^{-1}(w/u) = \tan^{-1}(x\lambda/zf'). \tag{24}$$

The value of the angle γ at the surface of the blade is found by taking the limit of equation (24) as $\eta \to 0$. Since λ and f' approach zero as $\eta \to 0$, it is convenient to expand $\lambda(\eta)_z$ and $f(\eta)$ as power series in η

$$f(\eta) = a_0 + a_1\eta + a_2\eta^2 + a_3\eta^3 + a_4\eta^4 + \ldots, \tag{25}$$

$$\lambda(\eta)_z = b_0 + b_1\eta + b_2\eta^2 + b_3\eta^3 + b_4\eta^4 + \ldots, \tag{26}$$

where the subscript on $\lambda(\eta)$ denotes at constant z. Equations (25) and (26) are subject to the boundary conditions

$$\left.\begin{aligned} f &= 0, \\ f' &= 0, \\ f'' &= 0{\cdot}33206, \\ \lambda &= 0, \end{aligned}\right\} \quad \text{at} \quad \eta = 0, \quad \lambda = 0 \quad \text{at} \quad \eta = \infty, \tag{27}$$

from which it follows that

$$a_0 = a_1 = b_0 = 0, \quad a_2 = \tfrac{1}{2}f''(0), \quad b_1 = \lambda'(0)_z. \tag{28}$$

Thus

$$\tan\gamma = \left(\frac{x}{z}\right)\left(\frac{\lambda'(0)_z + b_2\eta + b_3\eta^2 + b_4\eta^3 + \ldots}{f''(0) + 3a_3\eta + 4a_4\eta^2 + 5a_5\eta^3 + \ldots}\right), \tag{29}$$

and, on the surface of the blade at $\eta = 0$,

$$\tan\gamma_{\text{wall}} = \left(\frac{x}{z}\right)\left(\frac{\lambda'(0)_z}{f''(0)}\right). \tag{30}$$

Numerical calculations of the angle γ show that it is greatest at the wall. γ_{wall} increases linearly with increasing distance in the x-direction, and is inversely proportional to the radius.

The restrictions discussed in §2 imply that P and Q must be of order unity. Some representative solutions of equation (18) (for $P = 1$, $Q = -1$, 0 and $+1$) are given in figure 4.

4. Further properties of the differential equations

The differential equations (5), (6) and (7) were obtained on the assumptions that the mainstream velocity was a function of the radius only (i.e. $U = U(z)$), and that the stagger angle ψ was constant. Equation (18) was integrated numerically with respect to η (which is independent of z) by eliminating P and Q. The solutions will be more useful to designers of turbomachines if some radial variation in ψ can be accommodated, for they will then give an estimate of the boundary-layer flow on twisted blades. If $\psi = \psi(z)$, additional terms in $(d\psi/dz)$ will occur in the equations of motion as given in the appendix. It is found that the equations (5), (6) and (7) are unchanged if $(d\psi/dz)$ is of the order α, where $\alpha \ll 1$, so that the analysis given is valid for helical blades with small twist, the local values of ψ, P and Q being used in the solution of equation (18).

5. Discussion

Figure 4 shows the radial flow in the boundary layer for a fixed value of P, and varying values of Q. For no rotation, there is a radial flow inwards, the velocity attaining a maximum at $\eta = 1{\cdot}3$, although the maximum deviation of flow angle from the x-direction occurs at the wall.

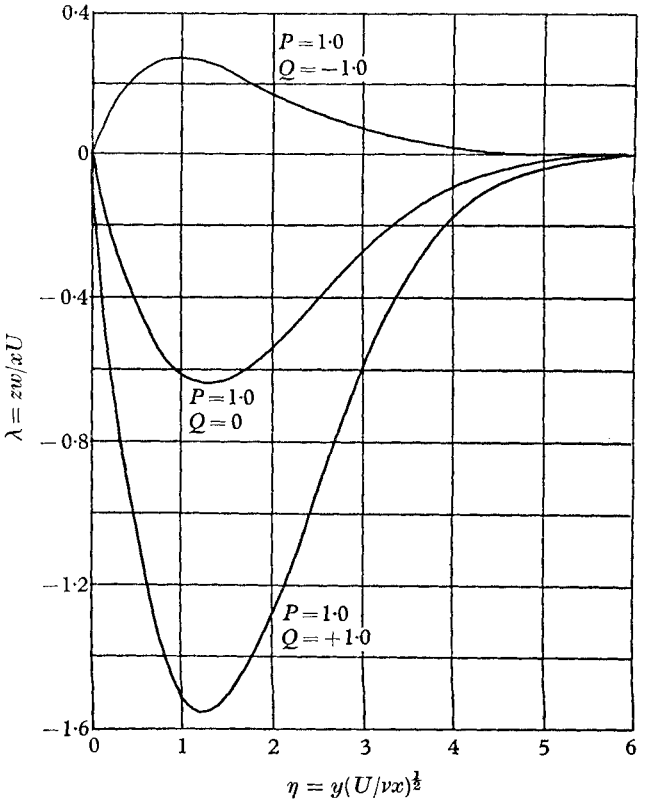

FIGURE 4. Some representative solutions of the equation in the radial direction.

When the circumferential component of the relative velocity and blade speed are in the same direction (as for most turbine rotor blades) the absolute circumferential velocity of the fluid near the blade is less than that in the mainstream, and there is a flow inwards along the blade in the boundary layer, as for $Q = 1{\cdot}0$ (figure 4). When the circumferential component of the relative velocity and the blade speed are in opposite directions, the absolute circumferential velocity of the fluid near the blade may be greater than that in the mainstream and there may be a flow outwards, as for $Q = -1{\cdot}0$ (figure 4). This usually occurs on compressor rotor blades.

The solution to Fogarty's problem of the rotating helicopter blade is obtained when $\psi = 90°$ and $U_b = z\Omega = -U$. There is no radial pressure gradient, since the absolute mainstream velocity, and hence the swirl, are zero. (In Fogarty's analysis the term (u^2/z) does not appear in the radial momentum equation because his

co-ordinate system, and therefore boundary conditions, are not the same as in the analysis given above.) Mager & Hansen's equation for the radial flow is identical with that for $g(\eta)$, equation (21). It is the case of $\psi = 90°$ and $U_b = 0$.

Appendix. The equations of motion in a helical co-ordinate system

In the appendix the following symbols are used:

$$\begin{aligned} c &\quad \cos\psi \\ s &\quad \sin\psi \\ \theta &\quad (x\sin\psi - y\cos\psi)/z \\ q &\quad u\sin\psi - v\cos\psi \\ \partial/\partial l &\quad \sin\psi(\partial/\partial x) - \cos\psi(\partial/\partial y) \\ \Delta^2 &\quad \frac{\partial}{\partial x^2} + \frac{\partial}{\partial y^2} + \frac{\partial}{\partial z^2}. \end{aligned}$$

The momentum equation in the x-direction:

$$\begin{aligned} &u\frac{\partial u}{\partial x} + v\frac{\partial u}{\partial y} + \frac{w}{(1+\theta^2)^{\frac{1}{2}}}\frac{\partial u}{\partial z} - \frac{ws}{z}\left\{\frac{w\theta^3}{(1+\theta^2)} - \frac{2q\theta^2}{(1+\theta^2)^{\frac{1}{2}}} - 2U_b(1+\theta^2)^{\frac{1}{2}}\right\} - \frac{(q+U_b)^2\theta s}{z} \\ &= -\frac{1}{\rho}\frac{\partial p}{\partial x} - \frac{\theta s}{\rho}\left(\theta\frac{\partial p}{\partial l} + \frac{\partial p}{\partial z}\right) + \nu\left[\Delta^2 u + \theta^2\left\{s\frac{\partial}{\partial l}\left(\frac{\partial u}{\partial x}\right) - c\frac{\partial}{\partial l}\left(\frac{\partial u}{\partial y}\right)\right\} + \frac{\theta}{z}\left(\sin 2\psi\frac{\partial v}{\partial l}\right.\right. \\ &\quad \left.\left. + \cos 2\psi\frac{\partial u}{\partial l}\right) + 2\theta\frac{\partial}{\partial l}\left(\frac{\partial u}{\partial z}\right) - \frac{s}{z^2}\left(q - \frac{2w\theta}{(1+\theta^2)^{\frac{3}{2}}}\right) + \frac{2\theta^2 s}{z(1+\theta^2)^{\frac{1}{2}}}\frac{\partial w}{\partial l} + \frac{1}{z}\frac{\partial u}{\partial z}\right]. \end{aligned} \tag{31}$$

The momentum equation in the y-direction:

$$\begin{aligned} &u\frac{\partial v}{\partial x} + v\frac{\partial v}{\partial y} + \frac{w}{(1+\theta^2)^{\frac{1}{2}}}\frac{\partial v}{\partial z} + \frac{wc}{z}\left(\frac{w\theta^3}{(1+\theta^2)} - \frac{2q\theta^2}{(1+\theta^2)^{\frac{1}{2}}} - 2U_b(1+\theta^2)^{\frac{1}{2}}\right) + \frac{(q+U_b)^2\theta c}{z} \\ &= -\frac{1}{\rho}\frac{\partial p}{\partial y} + \frac{\theta c}{\rho}\left(\theta\frac{\partial p}{\partial l} + \frac{\partial p}{\partial z}\right) + \nu\left[\Delta^2 v + \theta^2\left\{s\frac{\partial}{\partial l}\left(\frac{\partial v}{\partial x}\right) - c\frac{\partial}{\partial l}\left(\frac{\partial v}{\partial y}\right)\right\} + \frac{\theta}{z}\left(\sin 2\psi\frac{\partial u}{\partial l}\right.\right. \\ &\quad \left.\left. - \cos 2\psi\frac{\partial v}{\partial l}\right) + 2\theta\frac{\partial}{\partial l}\left(\frac{\partial v}{\partial z}\right) + \frac{c}{z^2}\left(q - \frac{2w\theta}{(1+\theta^2)^{\frac{3}{2}}}\right) - \frac{2\theta^2 c}{z(1+\theta^2)^{\frac{1}{2}}}\frac{\partial w}{\partial l} + \frac{1}{z}\frac{\partial v}{\partial z}\right]. \end{aligned} \tag{32}$$

The momentum equation in the z-direction:

$$\begin{aligned} &u\frac{\partial w}{\partial x} + v\frac{\partial w}{\partial y} + \frac{w}{(1+\theta^2)^{\frac{1}{2}}}\frac{\partial w}{\partial z} - \frac{w\theta}{z}\left(\frac{w\theta^3}{(1+\theta^2)^{\frac{3}{2}}} - q\frac{(1+2\theta^2)}{(1+\theta^2)} - 2U_b\right) - \frac{(q+U_b)^2}{z}(1+\theta^2)^{\frac{1}{2}} \\ &= -\frac{(1+\theta^2)^{\frac{1}{2}}}{\rho}\left(\theta\frac{\partial p}{\partial l} + \frac{\partial p}{\partial z}\right) + \nu\left[\Delta^2 w + \theta^2\left\{s\frac{\partial}{\partial l}\left(\frac{\partial w}{\partial x}\right) - c\frac{\partial}{\partial l}\left(\frac{\partial w}{\partial y}\right)\right\} - 2\frac{(1+\theta^2)^{\frac{1}{2}}}{z}\right. \\ &\quad \left.\times\left(s\frac{\partial u}{\partial l} - c\frac{\partial v}{\partial l}\right) + 2\theta\frac{\partial}{\partial l}\left(\frac{\partial w}{\partial z}\right) + \frac{\theta^2 w}{z^2}\frac{(2-\theta^2)}{(1+\theta^2)^2} + \frac{\theta}{z}\frac{(1+3\theta^2)}{(1+\theta^2)}\frac{\partial w}{\partial l} + \frac{1}{z}\frac{\partial w}{\partial z}\right]. \end{aligned} \tag{33}$$

The continuity equation:

$$\frac{\partial u}{\partial x} + \frac{\partial v}{\partial y} + \frac{1}{(1+\theta^2)^{\frac{1}{2}}}\frac{\partial w}{\partial z} + \frac{\theta^2}{(1+\theta^2)^{\frac{3}{2}}}\frac{w}{z} = 0. \tag{34}$$

REFERENCES

BLASIUS, H. 1908 *Z. Math. Phys.* **56**, 4.
FOGARTY, L. E. 1951 *J. Aero. Sci.* **18**, 247.
HOWARTH, L. 1938 *Proc. Roy. Soc.* A, **164**, 547.
MAGER, A. 1954 *J. Aero. Sci.* **21**, 835.
MAGER, A. & HANSEN, H. 1952 *N.A.C.A. Tech. Note* 2658.